J Heuristics (2006) 12: 73–94
DOI 10.1007/s10732-006-4983-4

Image registration with iterated local search*

Oscar Cordón · Sergio Damas

Submitted in May 2004 and accepted by Anthony Cox in September 2005 after 1 revision

Abstract This contribution is devoted to the application of iterated local search to image registration, a very complex, real-world problem in the field of image processing. To do so, we first re-define this parameter estimation problem as a combinatorial optimization problem, then analyze the use of image-specific information to guide the search in the form of an heuristic function, and finally propose its solution by iterated local search.

Our algorithm is tested by comparing its performance to that of two different baseline algorithms: *iterative closest point*, a well-known, image registration technique, a hybrid algorithm including the latter technique within a simulated annealing approach, a multi-start local search procedure, that allows us to check the influence of the search scheme considered in the problem solving, and a real coded genetic algorithm. Four different problem instances are tackled in the experimental study, resulting from two images and two transformations applied on them. Three parameter settings are analyzed in our approach in order to check three heuristic information scenarios where the heuristic is not used at all, is partially used or almost completely guides the search process, as well as two different number of iterations in the algorithms outer-inner loops.

Keywords Image registration · Iterated local search · Multi start local search · Genetic algorithms · Metaheuristics · Iterative closest point

*This work was partially supported by the Spanish Ministerio de Ciencia y Tecnología under project TIC2003-00877 (including FEDER fundings) and under Network HEUR TIC2002-10866-E.

O. Cordón
Department of Computer Science and A.I. University of Granada
e-mail: ocordon@decsai.ugr.es

S. Damas
Department of Software Engineering. University of Granada
e-mail: sdamas@ugr.es

1. Introduction

Image registration (IR) is a fundamental task in computer vision used for finding a correspondence (or transformation) among two or more pictures taken under different conditions: at different times, using different sensors, from different viewpoints, or a combination of these. Over the years, IR has been applied to a broad range of situations from remote sensing to medical images or artificial vision, and different techniques have been independently studied resulting in a large body of research. A clear classification of different IR techniques and applications is given in Brown (1992).

In the last few years, a new family of search and optimization algorithms have arisen based on extending basic heuristic methods by including them into an iterative framework augmenting their exploration capabilities. This group of advanced approximate algorithms has received the name *metaheuristics* (Glover and Kochenberger, 2003) and an overview of various existing methods is found in Blum and Roli (2003).

In recent literature, we can find different approaches to matching and IR problems from the metaheuristics point of view, specially considering genetic algorithms (GAs) (Yamany, Ahmed, and Farag, 1999; Han, Song, and Chung, 2001). Such interest in applying evolutionary techniques to IR is related to the fact that the most natural representation for the problem is the real coding of the involved parameters and the good behavior of GAs in parameter learning is well known.

In this work, we will tackle IR from a different perspective, that is, in terms of combinatorial optimization problems. To do so, we try to exploit the benefits of applying *Iterated Local Search (ILS)* (Lourenço, Martin, and Stützle, 2003) and our contributions are related to the fact of jointly solving matching and registration transformation problems in 3D using curvature derived information (Thirion and Gourdon, 1996). We both try to exploit the benefits of this information in order to reduce the number of meaningful points (the huge amount of data in the image makes it mandatory to select the most relevant ones prior to any other process) and to obtain a good topological characterization of the shape, therefore enabling a better matching.

In order to avoid the bias in our study, we develop a number of experiments. We will test the performance of our proposal based on ILS by comparing it with that of four different approaches: (i) a similar metaheuristic, Multi Start Local Search, (ii) a deterministic classical method (Iterative Closest Point (Liu, 2004)), (iii) a hybrid algorithm including the latter technique within a simulated annealing approach (Luck, Little, and Hoff, 2000), (iv) a genetic algorithm (Chow, Tsui, and Lee, 2004). These proposals tackle four different IR problems. A synthetic image as well as a real one are taken into account. Likewise, we will consider ten different runs of every experiment to avoid execution dependence.

In Section 2 we give some IR basics and we describe different approaches to solve that problem. In Section 3 we define the information we will take advantage of. Section 4 gives a brief introduction to ILS and analyzes the key concepts to apply it to the 3D IR problem. Next, Section 5 includes the performed experiments in order to compare our proposal to other approaches. Finally, in Section 6 we present concluding remarks and new open lines for future works.

2. Image registration

IR can be defined as a mapping between two images (I_1 and I_2, called scene and model, respectively) both spatially and with respect to intensity:

$$I_2(x, y, z, t) = g(I_1(f(x, y, z, t)))$$

The goal will be finding out the transformation that must be applied to the scene image in order to reach the model image. Therefore, we will match every pixel intensity value in I_2 (located in *(x,y,z)* at time *t*) with a pixel intensity value in I_1. Such a value will be obtained after applying a geometric transformation f to (x, y, z, t) and then a second intensity-based transformation g to the new location given by f.

We can usually find situations, where intensity difference is inherent to scene changes, and thus the intensity transformation estimation given by g is not necessary. In this contribution, we will consider both that the latter is the case (so no estimation of g is tackled) and that f represents a similarity transformation.

We can sort the different kinds of transformations f according to the maintenance (or not) of an established relation between geometric primitives (points, lines, etc.) in both the scene and the model, i.e., if f is a *similarity transformation*, every angle in the scene is preserved and the relative change in segment dimensions is the same in all directions, after applying it. Hence, a similarity transformation can be split in three ones: translation, rotation and uniform scaling. When dealing with 3D images, this implies that it involves seven parameters: translation (t_x, t_y, t_z), rotation $(\alpha_x, \alpha_y, \alpha_z)$ and uniform scaling S. Therefore, the parameters to be estimated in this contribution are those mentioned above.

The problem we are facing is especially hard as the amount of data to be managed is huge. *Feature based* registration methods solve this drawback by matching only the most relevant geometric primitives (points, lines, triangles, etc.) in both images. These primitives are the result of a preprocessing step of the intensity values of the pixels in the scene and the model images. Only the most significant data is to be studied, therefore reducing the problem complexity.

Although the final registration problem solution consists of the right values for the parameters which determine f, two different approaches arise, each of them working in a different solution space:

- To search for the optimal geometric primitive correspondence in the matching space and then identify the appropriate transformation parameters—using numerical methods such as least square estimation—to overlay the scene and the model considering such matching (Besl and McKay, 1992; Zhang, 1994; Fernández, Bardinet, and Damas, 2000; Bardinet, Fernández-Vidal, and Damas, 2000; Luck, Little, and Hoff, 2000; Liu, 2004), and
- To directly search in the parameter space (usually by means of evolutionary algorithms), computing the matching between scene and model geometric primitives to validate the estimated transformation once it has been applied (Simunic and Loncaric, 1998; Yamany, Ahmed, and Farag, 1999; Han, Song, and Chung, 2001; He and Narayana, 2002; Cordón, Damas, and Santamaría, 2003).

While the former involves determining which of the scene primitives match the model ones, the latter deals with the estimation of the registration transformation causing this model-scene overlapping.

Both approaches will be analyzed more deeply in what follows.

2.1. Search in the matching space

As said, the first possible approach is based on the following definition of the process objective: instead of searching for the parameters of a IR transformation, the goal is to minimize the global distance between each couple of paired points (primitives) in the scene and the model image. Hence, once the optimum matching between these images is achieved, we

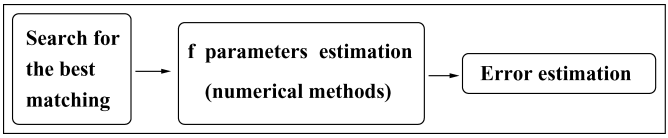

Fig. 1 Image registration problem solving as search in the matching space

can infer the implicit registration transformation by means of simple numerical optimization methods such as least squares estimation (Figure 1).

The complexity of the matching step and of the subsequent registration estimation depends on the method being considered. Likewise, an iterative process may be followed either for the estimation of the matching, or the registration transformation, or both. This is the case of the *Iterative Closest Point (ICP)* algorithm (Besl and McKay, 1992), and of other contributions (Zhang, 1994; Feldmar and Ayache, 1996; Fernández, Bardinet, and Damas, 2000; Bardinet, Fernández-Vidal, and Damas, 2000; Luck, Little, and Hoff, 2000; Liu, 2004).

Next, we will briefly describe the structure of the well known *ICP* algorithm in order to get a better understanding of the approach. The *ICP* method was proposed by Besl and McKay (1992), and later extended in different papers (Zhang, 1994; Feldmar and Ayache, 1996; Liu, 2004). ICP tries to achieve the best registration transformation f from the best matching of every geometric primitive in both scene and model images. Therefore, ICP follows the *search in the matching space* approach. Once the best matching is achieved, parameters related to the registration transformation f are obtained by means of simple numerical optimization methods.

Two images are the input to ICP: the scene image (I_1), defined by N_{I_1} points, and the model image (I_2), defined by N_{I_2} geometric primitives. The algorithm structure is as follows:

- The transformation f to be estimated is initialized to the identity $f_0 \leftarrow f_{\text{ident}}$, which does not change the points location. The number of iterations is also initialized: $k = 1$.
- The following steps are applied until convergence within a tolerance threshold $\tau > 0$:

1. The transformation estimated in the previous step is applied to the original scene I_1 to obtain a transformed scene $I_1^T \leftarrow f_{k-1}(I_1)$.
2. Every point in the transformed scene I_1^T is paired to the closest geometric primitive of the model image. The Mean Square Error in this iteration (MSE_k) is computed, showing the proximity of every point in the transformed scene I_1^T to the model I_2.
3. The transformation function f is updated by estimating the parameters related to f_k using a least square estimation. The function f will transform every scene point (in its original location I_1) to the place where it was matched to the geometric primitive of the model in the previous step.
4. The iteration is terminated if the change in Mean Square Error falls bellow a preset threshold $\tau > 0$ specifying a limit on the gain in each iteration: $|MSE_k - MSE_{k-1}| < \tau$.

The refered *Mean Square Error (MSE)* is a usual error measure in the field of IR typically given by:

$$MSE = \frac{\sum_{i=1}^{N} \| f(x_i) - y_i \|^2}{N}$$

where

- f is the estimated registration function.
- $x_i, i = 1, 2, \ldots, N_{I_1}$, are the N scene points (the registration function f is applied to every scene point).
- $y_i, i = 1, 2, \ldots, N_{I_2}$, are the N model points matching the scene ones.

ICP has several important drawbacks:

- It is sensitive to the presence of outliers.
- The initial states for the global matching play an essential role for the method's success when dealing with important deformations between model and scene points.
- The estimation of the initial states is not a trivial task.
- The cost of a local adjustment can be important if a low percentage of oclussion is present.

Hence, the algorithm performance is not good with transformations that have an important impact on the geometry of the images. As stated in Zhang (1994): "we assume the motion between the two frames is small or approximately known". This is a precondition of the algorithm to get reasonable results.

Our proposal is to improve ICP's matching results by adding heuristic information (curvature-derived information, see Section 3) to guide the ILS search process.

2.2. Search in the transformation parameter space

The second possibility involves directly searching for the solution to the registration problem in the space of the exact form of function f. To do so, the transformation function is usually parameterized and a coding scheme for the possible solutions representing values for these parameters is defined.

This way, the optimization procedure works by generating possible arrays of parameter values, i.e., possible registration functions f. To evaluate their goodness, the estimated transformation is applied to the scene points (or geometric primitives) and the distance between each transformed point and its closest point in the model image is computed. Of course, if the optimal transformation has been found, every point of the scene will overlap the corresponding in the model. However, if this is not the case, every point of the scene may fall at a distance d from its corresponding one in the model, thus clearly stating the problem of finding the best parameters defining f to minimize, in some way, the distance d (Figure 2).

Evolutionary Algorithms (Back, 1996) are usually the metaheuristic considered to put this approach into effect, as can be seen in view of the large number of contributions made (Simunic and Loncaric, 1998; Yamany, Ahmed, and Farag, 1999; Han, Song, and Chung, 2001; He and Narayana, 2002; Cordón, Damas, and Santamaría, 2003; Chow, Tsui, and Lee, 2004).

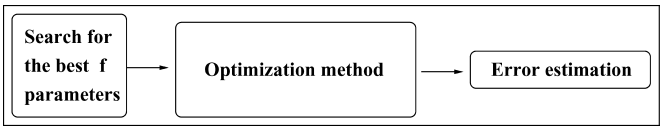

Fig. 2 Image registration problem solving as a search in the transformation parameter space

3. Shape derived heuristic information for 3D image registration

This section is devoted to introduce the information that can be derived from the shapes included in the images to be registered in order to better solve the IR problem. To do so, let us define the iso-intensity surface of a 3D image, which will be called simply the iso-surface in the rest of this paper. For any continuous function $C(x, y, z)$ of $\mathbb{R}^3$, any value I of $\mathbb{R}$ (called the iso-value) defines a continuous, not selfintersecting surface, without hole, which is called the iso-intensity surface of C (Monga, Benayoun, and Faugeras, 1992). A non ambiguous way to define the iso-surface is to consider it as being the surface which separates regions of the space where the intensity of C is greater or equal to I from those regions whose intensity is strictly lower than I. Whether such an iso-surface corresponds to the boundary of the scanned object or not is another problem, that will not be considered in the current contribution. In many cases, such as for medical images, iso-surface techniques are directly used to segment the organs, for example the bones in CT scans. In other applications, it is necessary to use iso-surface techniques as the final phase of the process to extract the surface in order to ensure that the reconstructed surfaces are continuous, not self-intersecting, and without hole (except of course for the image boundary). Because of those good topological properties, iso-surface techniques are the most widely used methods of segmentation for 3D medical images.

Let us see now some properties of the iso-surfaces (see Figure 3). At each point P of those surfaces, there is an infinite number of curvatures but, for each direction $\vec{t}$ in the tangent plane at P, there is only one associated curvature $k_{\vec{t}}$. There are two privileged directions of the surface, called the principal directions ($\vec{t}_1$ and $\vec{t}_2$), which correspond to the two extremal values of the curvature: k_1 and k_2.

One of these two principal curvatures is maximal in absolute value (let say k_1), and the two principal curvatures and directions suffice to determine any other curvature at point P. These differential values can be used in many different ways to locally characterize the surface. To those values, we can add the extremality criterion e as defined by Monga et al. in Monga, Benayoun, and Faugeras (1992), which is the directional derivative of the maximal curvature (let say k_1), in the corresponding principal direction ($\vec{t}_1$). In fact, the same extremality criterion can be also defined for the other principal direction, and we therefore have two "extremalities" e_1 and e_2. The locations of the zero-crossing of the extremality criterion define lines, which are called ridge lines or crest lines.

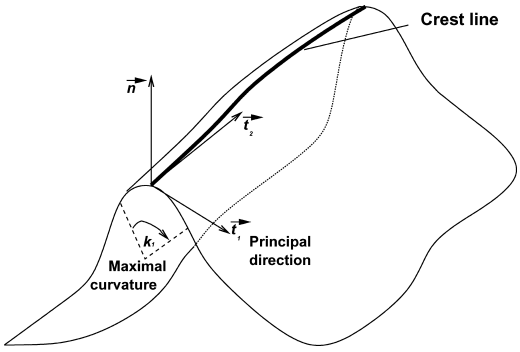

Fig. 3 Differential characteristics of surfaces

4. Iterated local search to solve 3d image registration

Iterated Local Search (ILS) (Lourenço, Martin, and Stützle, 2003) belongs to the group of metaheuristics that extend classical local search (LS) methods by adding diversification capabilities. This way, ILS is based on wrapping a specific LS algorithm by generating multiple initial solutions for it as follows:

procedure *Iterated Local Search*
  $s_0 =$ GenerateInitialSolution
  $s^* =$ LocalSearch(s_0)
  repeat
    $s' =$ Perturbation (s^*, $history$)
    $s^{*'} =$ LocalSearch(s')
    $s^* =$ AcceptanceCriterion(s^*, $s^{*'}$, $history$)
  until termination condition met
end

Hence, the algorithm starts by applying LS to an initial solution and iterates a procedure where a perturbation is applied to the current solution s^* in order to move it away from its local neighborhood, and the solution so obtained is then considered as the initial starting point for a new LS, resulting in another locally optimal solution $s^{*\prime}$. Then, a decision is made between s^* and $s^{*\prime}$ to decide from which solution the next iteration continues.

Once the general framework of ILS has been reviewed, the next sections introduce the different components considered to use this metaheuristic to solve the IR problem.

4.1. The local search algorithm considered

The LS procedure designed allows us to obtain a complete solution to the 3D registration problem, i.e., a point matching and a registration transformation.

The huge amount of data when dealing with 3D images makes it mandatory a selection of the most significant information. To do so, we take advantage of the curvature derived features (see Section 3) to be able to manage complex 3D surfaces. Therefore, in a preprocessing step, a 3D crest lines edge detector (Monga, Benayoun, and Faugeras, 1992) is applied to extract the most relevant feature points describing the surfaces.

Moreover, such a reduction allows us to guide the matching among different points, since we can take advantage of (k_1, k_2) principal curvatures and consider a good matching only if it is performed between points with similar principal curvature values.

Our proposal is based on solving the IR problem by searching in the matching space (see Section 2.1). So, a coding scheme specifying the matching between model and scene primitives (points in our case) has to be defined. Such matching is represented as a permutation π of size $N = \max(N_1, N_2)$, with N_1 and N_2 being the number of 3D points in the data and model shapes. Notice that this representation has two main pros:

- It is based on a permutation, a very common structure in the field (used for example to solve the traveling salesman and the quadratic assignment problems).
- It allows us to deal with the case when both images have a different number of points, thus automatically discarding outliers.

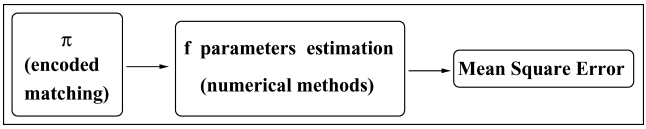

Fig. 4 MSE computation from a permutation π

Therefore, π stores a matching between both input images. We will be able to infer the parameters of the implicit registration transformation f related to π by means of simple numerical optimization methods such as least squares estimation (see Section 2.1). Once we know f, we can estimate the associated registration error. Figure 4 shows the global MSE computation from the given permutation π.

As said, the main novelty of our method is that the features of the image iso-surfaces (the curvature information seen in Section 3) are used to guide both the matching and the transformation estimation. So, we define a function $m_{\text{error}}(\cdot)$ evaluating the goodness of the matching stored in π by using (one of) the ridge measures shown in Section 3. In this contribution, we have chosen the following:

$$m_{\text{error}}(\pi) = \Delta k_1 + \Delta k_2 \quad \text{where} \quad \Delta k_j = \sum_{i=1}^{N} \left(k_j^i - k_j^{\pi_i}\right)^2, \qquad j = \{1, 2\}$$

Δk_1 and Δk_2 respectively measure the error associated to the matching of scene and model points with different values for the first and second principal curvatures.

This way, the fitness function (noted $F(\cdot)$) will include information regarding both previous criteria as follows:

$$\min\ F(\pi) \ = \ w_1 \cdot \sum_{i=1}^{N_1} \sum_{j=1}^{N_2} M_{ij} \|\vec{X}_i - \vec{t} - SR(\vec{\alpha})\vec{Y}_j\|^2 \ + \ w_2 \cdot m_{\text{error}}(\pi)$$

where the first term stands for the registration error: M is the binary matrix storing the matching encoded in π, and $(\vec{t}, \vec{\alpha}, S)$ are the similarity transformation parameters to be estimated—rotation, translation and scaling respectively—(see Section 2). The second one represents the matching error, and w_1, w_2 are weighting coefficients defining the relative importance of each.

With such function we will have a more suitable similarity measure to make a better search process in the space of solutions. Instead of considering a function based on a single registration error criterion, the use of the previous two terms working together to solve the IR problem, is an important part of our novel proposal.

Meanwhile, the neighborhood operator is the usual swapping, based on selecting two positions in π and exchanging their values. As the dimension of the problem makes it unmanageable the generation of the whole neighborhood to obtain the best neighbor, we will tackle the problem by searching for the first improving neighbor (first improvement), instead. The search process will stop either when none of the solutions in the neighborhood improves the current solution or when a prefixed number of first improvement iterations have been successful.

Finally, we should again note the strong importance of crest lines points not only to be used in order to reduce the matching domain, but also to characterize the global 3D isosurface

and to take advantage of the curvature derived information. Moreover, this will be a key point for the success of the proposal, as we will see later on.

4.2. The iterated local search components

The composition of the different ILS procedures is shown as follows:

- *GenerateInitialSolution:* A random permutation is computed.
- *Perturbation:* As a stronger change than the one performed by the swapping LS neighborhood operator is needed, we use a random exchange of the positions of the values included within a randomly selected sublist of size $\frac{N}{a}$, with $a \in \{2, 3, 4, 5, 6\}$ (the smaller the value of a, the stronger the perturbation applied).
- *AceptanceCriterion:* We directly select the best of s^* and $s^{*'}$ as current solution, which is shown to yield good performance for a variety of problems (Lourenço, Martin, and Stützle, 2003).
- *Termination condition:* The algorithm stops when a fixed number of iterations is reached.

5. Experiments and analysis of results

We present a number of experiments in order to study the performance of our proposal. As we will explain below, the experimental setup corresponding to these tests is as similar as possible since we wanted to extend our conclusions to other scenarios (new images, transformations, algorithms, etc.).

ILS results are compared both to classical IR methods and to similar metaheuristic approaches. On the one hand, a recent version of ICP is considered (Liu, 2004), as well as an hybrid approach combining ICP with a Simulated Annealing procedure (ICP+SA) (Luck, Little, and Hoff, 2000). On the other hand, Multi Start Local Search (MSLS) (Martí, 2003) and a real-coded dynamic GA (*DGA*) (Chow, Tsui, and Lee, 2004). ILS, MSLS and DGA are heuristic search procedures that aspire to find globally optimal solutions to hard combinatorial optimization problems.

5.1. Experimental design

This subsection is devoted to describe the experiments developed to estimate several registration transformations in two different 3D images. For the sake of clarity, it has been divided into three different parts. First, the two basic 3D images considered are presented. Then, two different transformations applied to both are introduced. Finally, we deal with the parameter settings for the ILS algorithm.

5.1.1. Model and scene images

Our results correspond to a number of registration problems for two different 3D images (one is synthetic, the other is a magnetic resonance image —MRI—). Both have suffered the same two global similarity transformations which must be estimated by the ILS algorithm described in this paper. Because of the amount of data to be managed, it is necessary to carry out a preprocessing step in order to extract a set of feature points which describe the surfaces. Crest line points are obtained from the images of a superellipsoid and a brain, returning 222

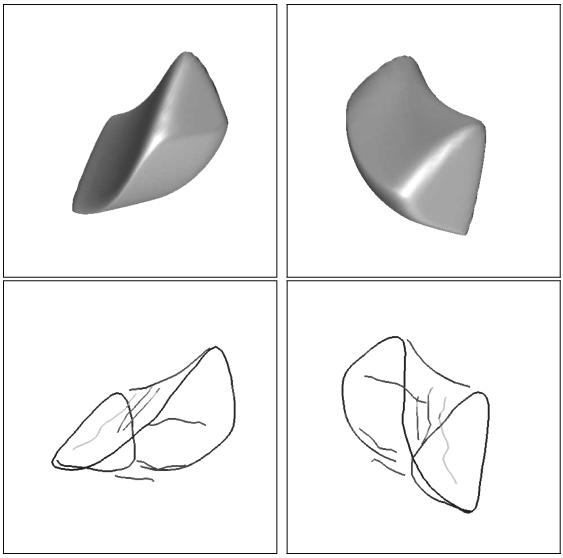

Fig. 5 Different views of the 3D "Piece of cheese" image (first row) and their respective crest lines points (second row)

and 1052 points respectively. We will refer to each of them as the "Piece of cheese" and "Brain" images. Both original and preprocessed images are presented in Figures 5 and 6.

5.1.2. Transformations to be estimated

Our tests are based on the estimation of the parameters of two different similarity functions. Such transformations are stored in Table 1 and can be appreciated when being applied to one of the objects in Figure 7, where different colors have been used to distinguish the scene (dark gray) and the model (light gray). In such tables (and from now on), all the different

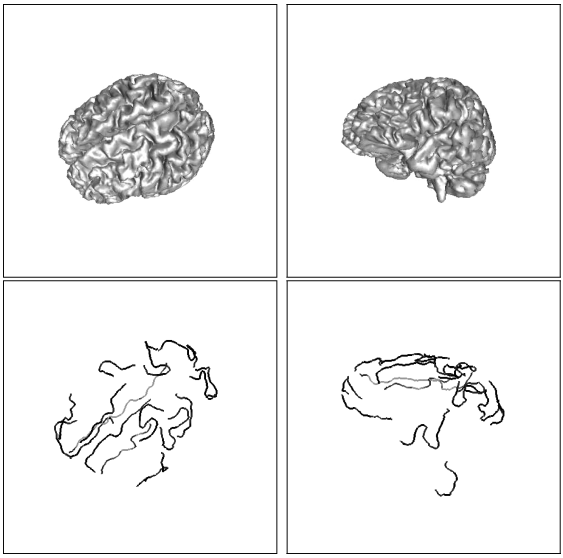

Fig. 6 Different views of the 3D "Brain" image (first row) and their respective crest lines points (second row)

Table 1 Transformations applied to each of the two 3D images

Tr. no.	$RAngle^{\circ}$	$RAxis_x$	$RAxis_y$	$RAxis_z$	Δ_x	Δ_y	Δ_z	S
1	180.6	−0.11547	0.80829	−0.57735	−7.5	−12	10.8	1.5
2	202.5	−0.536895	0.59655	0.59655	24.0	10.6	5.2	2.0

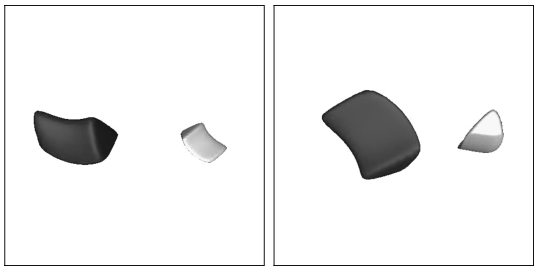

Fig. 7 The two transformations to be estimated (Table 1) are shown when applied to the first object ("Piece of cheese")

3D rotations have been expressed in terms of rotation angle ($RAngle^{\circ}$) and rotation axis ($RAxis_x, RAxis_y, RAxis_z$) instead of using other representations (Euler angles, for instance). This way, we will achieve a better understanding of the geometric transformation involved.

5.1.3. Testing algorithms

ILS results will be compared to those obtained by a similar metaheuristic approach, MSLS (Martí, 2003). Other state of the art proposals are also considered. On the one hand, a recent version of a classical IR method, ICP (Liu, 2004), is tested. Likewise, the performance of an hybrid approach combining ICP with a Simulated Annealing procedure (ICP+SA) (Luck, Little, and Hoff, 2000) is analyzed. Finally, an evolutionary algorithm (DGA) (Chow, Tsui, and Lee, 2004) is studied. Therefore, the following analysis of results is structured considering first the test image (either "Piece of cheese" or "Brain"), and the testing algorithm (two comparisons will be established *MSLS vs. ILS,* and *ICP, ICP+SA, DGA vs. ILS*).

In order to achieve a better comprehension of the results, we present both the *MSE* value and the *percentage of perfect matchings* of every solution as metrics to compare MSLS and ILS. This percentage corresponds to the number of correct matchings coded in the final permutation. Nevertheless, ICP, ICP+SA and DGA results are analyzed in terms of MSE only, since these methods do not maintain a solution representation based on matching.

5.1.4. Parameter settings

In the experiments, we have considered various parameter values to test the algorithms performance in different conditions. Hence, the ILS and MSLS algorithms were run for 20 and 50 iterations, considering different values for the maximum number of iterations in the LS loop (1000 and 2500). Considering the permutation size (several hundreds of elements) involved in every IR problem, we need a perturbation operator able to avoid local optima. Likewise, a preliminar study showed that the stronger the perturbation the better the ILS performance. Hence, the parameter a has been set to 2. The weights in the objective function have been defined as $w_1 = w_1'$ and $w_2 = w_2' \cdot \frac{m_{\text{error}}(\pi_0)}{MSE(f_0)}$, with $m_{\text{error}}(\pi_0)$ and $\text{MSE}(f_0)$ being respectively the matching and registration errors of the initial solution, in order to get a

uniform measure of both the matching error (curvature-derived error) and the registration error (MSE). Different settings of w_1' and w_2' have also been tested in order to balance the influence of the MSE and the curvature in the final solution.

On the other hand, the *DGA* works with 500 individuals and with 300 scene image points, as indicated in Chow, Tsui, and Lee (2004). Meanwhile, the hybrid algorithm (ICP+SA) also considers a maximum number of 40 iterations for ICP and 30 iterations for the annealing, as well as 50 trial movements around each annealing iteration. In order to guarantee a proper convergence of these algorithms (avoiding a premature stop), they are run for the same time than ILS in every problem instance, i.e., 80 sec. for the "Piece of cheese" image and 12 min. for the "Brain" image.

All the runs have been performed on a 2200 MHz. Pentium IV processor computer. Finally, it is worth noting that, in order to avoid execution dependence, all the statistics presented below correspond to ten different runs of every algorithm and transformation with a different seed (but ICP which is a deterministic method).

5.2. Analysis of results

5.2.1. Results

Tables 2, 3, 4 and 5 show the results obtained for the "Piece of cheese" (Tables 2 and 3) and "Brain" (Tables 4 and 5) objects, when facing the two IR problems presented in Table 1. These tables are structured as follows:

- **The first row** shows the algorithms to be compared. That is: ILS vs. MSLS (the remaining results will be presented in a later section).
- **The second row** includes the different number of iterations considered in either the inner LS loop (2500 and 1000) and the outer ILS or MSLS loop (20 and 50). For example, 20×2500 means 20 iterations of the outer loop, each of them composed of a LS with a maximum number of 2500 iterations.
- **The third row** shows the error estimation parameters to be used in the proper study of the results. Both MSE and the percentage of perfect matchings (%) are essential for the right interpretation of a solution. An isolated low MSE value could represent a local optimum matching where most of the points would not be properly matched. Such a situation is avoided when adding the % information.
- **Three sets of three rows** corresponding to three different settings of w_1' and w_2': (0.1, 0.9), (0.5, 0.5) and (1, 0). These values let us study the influence of curvature derived information in achieving good solutions. Hence, the settings range from the maximum weight for the curvature information ($w_2' = 0.9$) and the only attention to the MSE in the objective function, avoiding curvature information ($w_2' = 0$). Every set of three rows shows the minimum, mean and variance of the ten runs.
- Finally, we remark the best absolute and average values in these four tables **using bold font**.

Finally, in this section we also show figures that are helpful to understand the best solutions achieved by every studied algorithm. In these figures, scene images are transformed by the mentioned solution and the result is presented (in dark gray) together with the model (in light gray). The better the estimation, the closer the dark and light gray objects.

Table 2 MSE and percentage of perfect matchings corresponding to the first transformation in Table 1 applied to the "Piece of cheese" image

	"PIECE OF CHEESE": TR. 1							
	MSLS				ILS			
	20 × 2500		50 × 1000		20 × 2500		50 × 1000	
	MSE	%	MSE	%	MSE	%	MSE	%
(0.1, 0.9)								
Min.	0.93	38.74	34.39	7.66	$\simeq$ **0**	**90.54**	$\simeq$ **0**	86.04
Mean	2.16	31.08	73.18	3.78	22.80	55.05	**7.38**	**70.81**
σ^2	1.83	4.18	17.43	1.70	34.68	31.36	21.88	20.88
(0.5, 0.5)								
Min.	0.34	45.05	6.30	12.16	0.61	67.57	0.57	54.05
Mean	17.02	22.34	35.74	6.53	35.73	32.75	54.03	17.97
σ^2	31.94	11.25	25.84	3.12	43.28	24.68	35.56	21.53
(1, 0)								
Min.	5.57	12.61	1.56	9.46	40.41	0.90	39.27	0.90
Mean	35.91	3.83	28.47	3.47	55.15	0.32	51.08	0.45
σ^2	21.72	4.11	17.36	3.22	9.11	0.29	7.14	0.35

Table 3 MSE and percentage of perfect matchings corresponding to the second transformation in Table 1 applied to the "Piece of cheese" image

	"PIECE OF CHEESE": TR. 2							
	MSLS				ILS			
	20 × 2500		50 × 1000		20 × 2500		50 × 1000	
	MSE	%	MSE	%	MSE	%	MSE	%
(0.1, 0.9)								
Min.	1.04	46.85	57.63	10.81	$\simeq$ **0**	**90.54**	$\simeq$ **0**	86.04
Mean	2.92	33.47	139.85	2.97	40.85	53.33	**12.86**	**69.91**
σ^2	1.64	7.63	37.43	2.85	62.11	29.99	38.22	20.80
(0.5, 0.5)								
Min.	0.61	45.05	27.53	10.36	0.75	61.26	0.98	51.80
Mean	11.99	23.87	75.32	6.62	71.72	24.41	101.73	16.62
σ^2	9.77	8.56	47.72	2.65	72.48	21.38	68.07	20.53
(1, 0)								
Min.	9.90	12.61	2.32	11.26	72.29	0.45	78.86	0.90
Mean	56.61	3.60	28.64	5.77	97.15	0.32	91.01	0.36
σ^2	34.42	4.36	23.58	3.33	17.12	0.21	11.90	0.27

Table 4 MSE and percentage of perfect matchings corresponding to the first transformation in Table 1 applied to the "Brain" image

	"BRAIN": TR. 1							
	MSLS				ILS			
	20 × 2500		50 × 1000		20 × 2500		50 × 1000	
	MSE	%	MSE	%	MSE	%	MSE	%
(0.1, 0.9)								
Min.	67.65	0.86	1166.38	0.29	**0.85**	**28.90**	5.96	13.12
Mean	1284.80	0.32	1492.50	0.10	**140.33**	**16.43**	332.78	7.01
σ^2	457.94	0.22	210.83	0.10	274.39	8.98	395.29	5.30
(0.5, 0.5)								
Min.	155.73	0.57	456.54	0.57	10.59	13.31	39.72	6.37
Mean	1119.92	0.19	1156.58	0.13	438.30	4.74	581.37	2.01
σ^2	458.75	0.17	371.80	0.17	296.66	5.13	295.97	2.15
(1, 0)								
Min.	7.61	1.05	112.22	0.10	3.70	12.45	12.85	8.46
Mean	101.98	0.30	527.80	0.06	281.35	6.10	547.95	1.95
σ^2	190.28	0.27	314.76	0.05	338.84	5.18	457.29	2.76

Table 5 MSE and percentage of perfect matchings corresponding to the second transformation in Table 1 applied to the "Brain" image

	"BRAIN": TR. 2							
	MSLS				ILS			
	20 × 2500		50 × 1000		20 × 2500		50 × 1000	
	MSE	%	MSE	%	MSE	%	MSE	%
(0.1, 0.9)								
Min.	2514.42	0.57	1854.36	0.19	**1.33**	**23.38**	4.75	13.50
Mean	2786.14	0.25	2732.62	0.07	**125.55**	**17.90**	552.85	7.02
σ^2	220.43	0.18	449.26	0.07	361.87	6.22	657.02	5.33
(0.5, 0.5)								
Min.	132.07	3.14	862.58	0.38	18.52	10.46	58.31	6.37
Mean	836.18	0.77	2089.18	0.18	769.46	3.19	1035.28	2.55
σ^2	860.16	0.89	547.78	0.12	518.76	3.86	743.09	2.48
(1, 0)								
Min.	32.39	0.67	218.76	0.38	5.05	12.07	13.87	8.65
Mean	701.99	0.10	864.16	0.17	453.16	5.84	730.76	2.94
σ^2	645.74	0.19	471.15	0.12	539.07	5.09	818.01	3.26

5.2.2. Analysis of results for the "piece of cheese" image

MSLS: When analyzing the results obtained by MSLS in both the first and second transformations (left side of Tables 2 and 3), we realize that:

- The heuristic information considered by the search process, i.e., the curvature information (represented by $(w'_1, w'_2) = (0.1, 0.9)$), is relevant in order to achieve reasonable solutions. Best mean MSLS results (and some absolute minima) correspond to this parameter setting. The same stands for the percentage of perfect matchings.
- When dealing with the number of iterations of inner and outer MSLS loops, the "20×2500" scenario outperforms the "50×1000" one if heuristic information is taken into account. Hence, when no information from previous solutions is considered to explore the search space, a higher number of iterations of the LS is needed to achieve better solutions.

ILS: Attending to the ILS results collected in the right sides of Tables 2 and 3, we conclude that:

- The curvature information (represented by $(w'_1, w'_2) = (0.1, 0.9)$) is essential to achieve good solutions. Both the best mean ILS results and the best absolute minima correspond to this parameter setting. We remark the importance of this heuristic information when we analyze the percentage of perfect matchings that ranges from $\simeq 90\%$ when $w'_2 = 0.9$, to $\simeq 0.9\%$ when no curvature derived information is considered ($w'_2 = 0$).
- When dealing with the number of iterations of the inner and outer ILS loops, 1000 iterations in the LS seem to be enough to achieve intermediate solutions of high quality. Such solutions are useful to explore the search space. Notice that this aspect differs from the MSLS results as the better diversification-intensification trade-off of ILS allows it to be able to generate better solutions with a larger number of starting points and a smaller number of LS iterations. Best mean ILS results are obtained in both transformations considering "50×1000" iterations (although the best IR absolute estimations are obtained when "20×2500" iterations are considered).
- If we compare the results of both, we realize that ILS clearly outperforms MSLS:

  1. As regards the robustness of the algorithms, the average results in the 10 runs performed show that the best mean ILS estimations are approx. 70% perfect matchings, while mean MSLS ones are 33% perfect matchings.
  2. With respect to the best absolute solutions, ILS ones are around 90% of perfect matchings, while MSLS ones are just about 45% perfect matchings.
  3. Only when the curvature information is not considered, $(w'_1, w'_2) = (1, 0)$, MSLS outperforms ILS. However, as mentioned before, the results obtained when using heuristic information are always significantly better in both algorithms. Hence, such information is essential for a good behavior in IR solving.
  4. Figure 8 shows the best absolute estimations achieved by MSLS (left column) and ILS (right column). We appreciate that there is no perfect overlap between the light and dark grey objects for MSLS, which suggests a lower performance of the algorithm in the two estimations. On the other hand, ILS solutions are so good that one can not distinguish between the scene object transformed by such solutions (in dark gray) and the model object (in light gray).
  5. As regards the average run time of the two algorithms, it is the same when considering "20×2500" iterations: 33 sec. Nevertheless, the average run time of MSLS with "50×1000" iterations ranges from 41 sec. (if curvature information is considered) to 1min. (if no curvature is taken into account). Meanwhile, ILS one is always 1 min.18 sec.

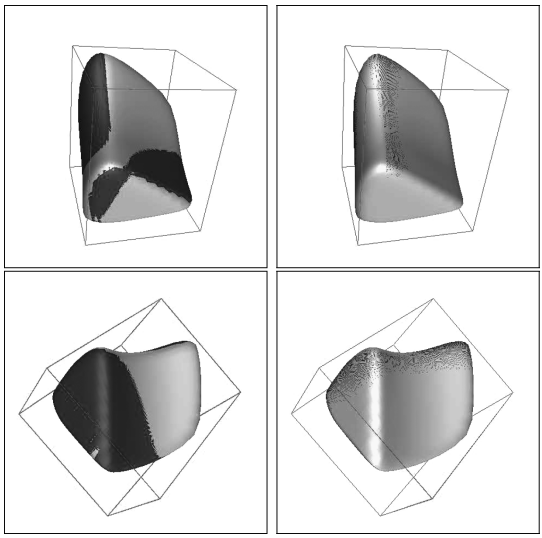

Fig. 8 MSLS vs. ILS results when dealing with the first two IR problems ("Piece of cheese" image with transformations TR1 -upper row- and TR2 -lower row–). The higher the overlap, the better the solution. First column: MSLS estimations. Second column: ILS estimations

Therefore, ILS needs some additional time to explore the search space and to achieve a better result.

5.2.3. Analysis of results for the "Brain" image

MSLS: When facing this IR problem of higher complexity, MSLS results (left sides of Tables 4 and 5) show that:

- All the estimations are much worse than those obtained in the "Piece of cheese" image. Mean and best MSE values are almost always around several hundreds, while the percentage of perfect matchings is usually below 1%.
- The curvature information does not seem to be really relevant in these estimations (especially in the second transformation). They are all really poor and such a situation shows that heuristic information is not properly taken into account.
- LS would need of a high number of iterations to solve this complex problem. Therefore, the results corresponding to the "20 × 2500" scenario usually outperform those from the "50 × 1000" one (in all cases but in the $w1' = 0.1, w2' = 0.9$ combination for transformation TR2).

ILS: With respect to the ILS results shown in the right sides of Tables 4 and 5, we conclude:

- Again, all the estimations are worse than those obtained in the "Piece of cheese" image, because of the complexity of the new problem instances. Nevertheless, ILS outputs are good enough to achieve accurate IR estimations.
- The curvature information (represented by $(w_1', w_2') = (0.1, 0.9)$) is essential to achieve good solutions. The best mean ILS results and the best absolute minima correspond to this parameter setting in both transformations.
- As seen in the MSLS analysis, it seems that the LS procedure needs a high number of iterations to solve this complex problem. Therefore, the results corresponding to "20 × 2500" iterations always outperform those of "50 × 1000" iterations.

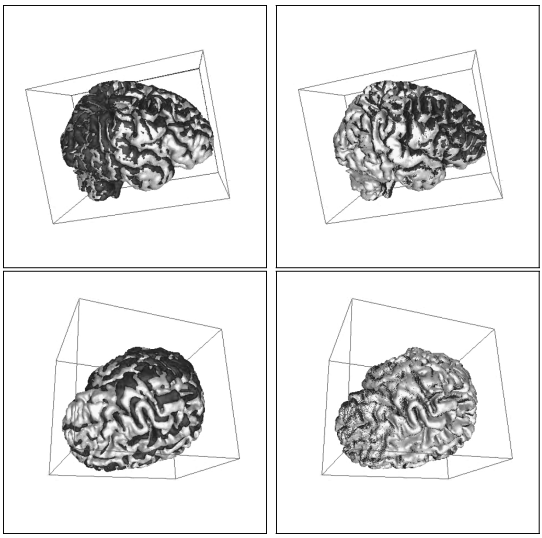

Fig. 9 MSLS vs. ILS results when dealing with the two IR problems ("Brain" image with transformations TR1 –upper row and TR2 –lower row). The higher the overlap, the better the solution. First column: MSLS estimations. Second column: ILS estimations

– If we compare these results to those obtained by MSLS, we conclude that ILS clearly outperforms MSLS and:

1. Considering robustness, the best mean ILS estimations are 17% of perfect matchings, while mean MSLS ones are just of 0.5% of perfect matchings.
2. According to the best solutions, ILS gives around 25% of perfect matchings, while MSLS ones are only a 1% of perfect matchings.
3. Figure 9 shows the best absolute estimations achieved by MSLS and ILS. The first row corresponds to the MSLS estimations. We appreciate that there is no perfect overlap between the dark and light grey objects, which suggests the low performance of the algorithm in the two estimations. On the other hand, ILS solutions are again so good that it is impossible to distinguish between the scene object transformed by such solutions (in dark grey) and the model one (in light grey).
4. As regards the run time of the two algorithms, Table 6 shows the minimum, average and variance values for the ten runs performed. The behavior of both algorithms is the same in the two transformations: ILS needs roughly the double of time to reach much better results than MSLS. Hence, MSLS minimum and average run times are lower than ILS ones in every experiment but, as we have stated above, ILS clearly outperforms MSLS achieving higher quality solutions. It is worth noting the robustness of the MSLS run time: nine of the twelve variance values are less than or equal to 11 seconds. Finally, the highest quality solutions in both transformations (achieved by ILS when $(w1', w2') = (0.1, 0.9)$ and 20×2500 iterations are considered) need 12 min,3 sec. and 11 min,58 sec. on average respectively (these results have been highlighted in Table 6 using bold font).

5.2.4. ILS vs. IR state of the art methods

This section is devoted to the study of the behavior of state of the art IR methods (ICP, ICP + SA, DGA) with respect to our proposed ILS approach.

Table 6 "Brain" image: run time of the different solutions (in seconds)

"BRAIN": RUN TIME								
	MSLS				ILS			
	20 × 2500		50 × 1000		20 × 2500		50 × 1000	
	TR1	TR2	TR1	TR2	TR1	TR2	TR1	TR2
(0.1, 0.9)								
Min.	217	214	204	204	540	545	471	471
Mean	223	222	205	205	**723**	**718**	577	571
σ^2	5	5	1	1	118	106	72	62
(0.5, 0.5)								
Min.	379	374	315	324	668	666	659	660
Mean	397	400	335	336	852	840	806	818
σ^2	10	15	11	8	104	106	103	113
(1, 0)								
Min.	334	334	371	373	519	515	599	619
Mean	347	353	408	401	743	717	832	869
σ^2	8	11	20	22	152	140	169	180

ICP vs. ILS: The results collected in Tables 7 and 8 show not only that ILS clearly outperforms ICP in terms of MSE, but also the high quality of the ILS estimations. If they are compared to the global optimum stored in Table 1, both ICP and ILS achieve good translation and scaling estimations, but only ILS is able to give an accurate rotation estimation. In fact, orders of magnitude in the scale of f parameters are crucial when solving the registration problem. Unit changes in angle have a much greater impact on an image than unit changes in translation. This difference in scale appears as elongated valleys in the parameter search space causing difficulties for the traditional local optimizers (Besl and McKay, 1992; He and Narayana, 2002).

As we stated in Section 2.1, ICP performance is not good when dealing with transformations that have an important impact in the geometry of the images (like TR1 and TR2, considered in this proposal).

Table 7 ICP and ILS estimations of the "Piece of cheese" image transformations

"PIECE OF CHEESE": ICP vs. ILS								
$RAngle^\circ$	RAx_x	RAx_y	RAx_z	Δ_x	Δ_y	Δ_z	S	**MSE**
			ICP					
13.97°	0.34	−0.14	0.93	−9.17	−22.88	2.61	1.21	139.7
44.18°	−0.54	0.52	0.67	22.16	19.96	3.74	1.41	302.5
			ILS					
180.59°	−0.114641	0.808509	−0.577209	−7.5	−12	10.8	1.5	$\simeq 0$
202.59°	−0.536736	0.596819	0.596424	24.0	10.6	5.2	2.0	$\simeq 0$

Table 8 ICP and ILS estimations of the "Brain" image transformations

"BRAIN": ICP vs. ILS								
$RAngle^{\circ}$	RAx_x	RAx_y	RAx_z	Δ_x	Δ_y	Δ_z	S	**MSE**
			ICP					
323.36°	0.89	0.41	0.22	9.01	−21.94	74.27	0.72	6016.10
322.91°	−0.73	−0.05	0.68	54.74	1.02	18.27	0.92	6535.40
			ILS					
180.29°	−0.113511	0.805279	−0.581928	−7.5	−12	10.8	1.5	0.85
202.52°	−0.541293	0.597655	0.591449	24.0	10.6	5.2	2.0	1.33

Table 9 ICP+SA and ILS MSE values of the "Piece of cheese" and "Brain" IR solutions.

	"PIECE OF CHEESE"					**"BRAIN"**				
	ICP+SA			*ILS*		*ICP+SA*			*ILS*	
	Min.	Max.	Mean	S. dev.	Min.	Min.	Max.	Mean	S. dev.	Min.
TR1	56.5	103.4	87.4	16.2	$\simeq 0$	4798.8	5076.6	4952	102.4	0.85
TR2	163.5	198.6	176.9	11.3	$\simeq 0$	6304.7	6535.4	6475.1	87.4	1.33

Table 10 DGA and ILS MSE values of the "Piece of cheese" and "Brain" IR solutions

	"PIECE OF CHEESE"					**"BRAIN"**				
	DGA			*ILS*		*DGA*			*ILS*	
	Min.	Max.	Mean	S. dev.	Min.	Min.	Max.	Mean	S. dev.	Min.
TR1	42.6	143	66.9	27.1	$\simeq 0$	569.7	2645.2	1258.7	651	0.85
TR2	89.4	229	154.3	40.6	$\simeq 0$	1089.1	2717.9	1858.5	493.9	1.33

ICP+SA vs. ILS: ICP+SA solutions are better than those achieved by ICP. Nevertheless, the results collected in Table 9 show that ILS still significantly outperforms ICP+SA, regarding to both average and minimum ICP+SA MSE values.

DGA vs. ILS: After performing this experimental setup, we have recognized that DGA is the best of the state of the art algorithms considered. However, the results in Table 10 again show that ILS clearly outperforms DGA, regarding to both average and minimum MSE values.

Figures 10and 11 show the best absolute estimations achieved by the state of the art algorithms considered (i.e. DGA), as well as the baseline ICP ones, with respect to ILS. Since DGA solutions are worse than those from MSLS, it is easier to understand these graphics. The first row of every figure corresponds to the DGA estimations. We appreciate that there is no overlap at all between the dark and light gray objects, which suggests the low performance of the algorithm in the four estimations involved. On the other hand, ILS solutions are so good that it is impossible to distinguish between the scene object transformed by such solutions (in dark gray) and the model (in light gray).

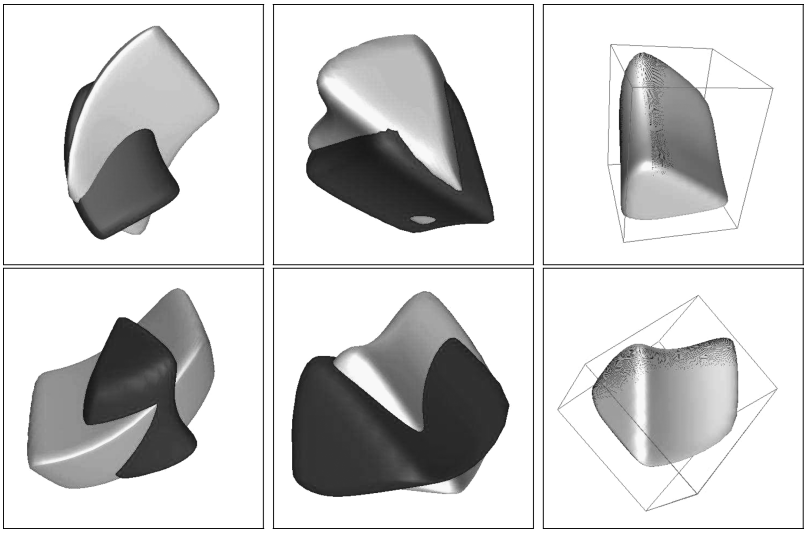

Fig. 10 ICP and DGA vs. ILS results when dealing with the two IR problems ("Piece of cheese" image). The higher the overlapping, the better the solution. First column: ICP estimations of TR1 and TR2. Second column: DGA estimations of both transformations. Third column: ILS results

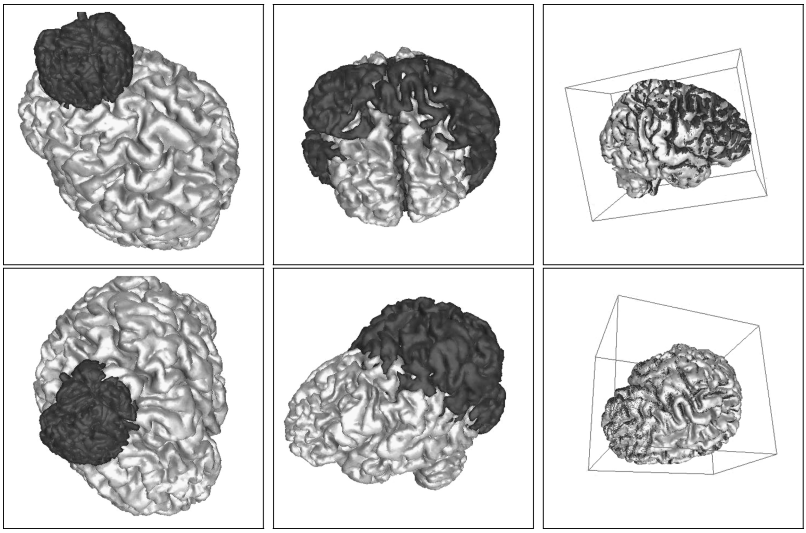

Fig. 11 ICP and DGA vs. ILS results when dealing with the two IR problems ("Brain" image). The higher the overlapping, the better the solution. First column: ICP estimations of TR1 and TR2. Second column: DGA estimations of both transformations. Third column: ILS results

6. Concluding remarks and future work

In this contribution, we have formulated the IR problem as a two fold one in order to jointly solve the matching and the search for the similarity parameters of the registration transformation. To do so, we take advantage of the information inferred from the principal curvatures of

the crest lines points. We use the ILS metaheuristic to face such a complex optimization task. We have presented different results considering synthetic and real-world images together with transformations that greatly affect the geometry of the images. We show how the ILS solutions outperform those obtained by the MSLS similar metaheuristic and other state of the art methods in the IR field: ICP, ICP + SA and DGA.

There is a number of new open lines to be followed. On the one hand, it is necessary a deeper study on the 3D IR ILS technique behavior when dealing with different error situations. Moreover, it would be interesting to study the behavior of other metaheuristics when dealing with the registration problem. Hence, ant colony optimization (Dorigo and Stützle, 2003) and scatter search (Laguna and Martí, 2003) metaheuristics seem to be good candidates.

Acknowledgments The authors would like to thank the anonymous referees for their valuable comments that allowed them to highly improve the paper quality.

References

T. Bäck. (1996). *Evolutionary Algorithms in Theory and Practice*. Oxford University Press.

Bardinet, E., S. Fernández-Vidal, S. Damas, G. Malandain, and N. Pérez de la Blanca. (2000). "Structural Object Matching." In *Proceedings of the 2nd International Symposium on Advanced Concepts for Intelligent Vision Systems (ACIVS 2000)* 2, Germany: Baden-Baden, pp. 73–77.

Besl, P.J. and N.D. McKay. (1992). "A Method for Registration of 3-D Shapes." *IEEE Transactions on Pattern Analysis and Machine Intelligence* 14, 239–256.

C. Blum and A. Roli. (2003). "Metaheuristics in Combinatorial Optimization: Overview and Conceptual Comparison." *ACM Computing Surveys* 35(3), 268–308.

Brown, L.G. (1992). "A Survey of Image Registration Techniques." *ACM Computing Surveys* 24(4), 325–376,

C. K. Chow, Tsui, H.T. and T. Lee. (2004). "Surface Registration Using a Dynamic Genetic Algorithm." *Pattern Recognition* 37, 105–117.

Cordón, O., S. Damas, and J. Santamaría. (2003). "A CHC Evolutionary Algorithm for 3D Image Registration." In T. Bilgic, B.D. Baets, and O. Bogazici, (eds.), *Lecture Notes in Artificial Intelligence 2715*, Springer, pp. 404–411.

Dorigo, M. and T. Stützle. (2003). "The Ant Colony Optimization Metaheuristic: Algorithms, Applications, and Advances." In F. y Glover, G. Kochenberger, (eds.), *Handbook of Metaheuristics*, Kluwer Academic Publishers, pp. 251–285.

Feldmar, J. and N. Ayache. (1996). "Rigid, Affine and Locally Affine Registration of Free-Form Surfaces." *International Journal of Computer Vision* 18(2), 99–119.

S. Fernández-Vidal, E. Bardinet, S. Damas, G. Malandain, and N. Pérez de la Blanca. (2000). "Object Representation and Comparison Inferred From Its Medial Axis." In *Proceedings of the International Conference on Pattern Recognition (ICPR 00)* Spain: Barcelona, 1, pp. 712–715.

F. Glover and G. Kochenberger. (2003). *Handbook of Metaheuristics*. Kluwer Academic Publishers.

Han, K.P., K.W. Song, E.Y. Chung, S.J. Cho, and Y.H. Ha. (2001). "Stereo Matching Using Genetic Algorithm With Adaptive Chromosomes." *Pattern Recognition* 32, 1729–1740,

He, R. and P.A. Narayana. (2002). "Global Optimization of Mutual Information: Application to Three-Dimensional Retrospective Registration of Magnetic Resonance Images." *Computerized Medical Imaging and Graphics* 26, 277–292.

Laguna, M. and R. Martí. (2003). *Scatter Search: Methodology and Implementations in C*. Kluwer Academic.

Liu, Y. (2004). "Improving ICP With Easy Implementation for Free Form Surface Matching." *Pattern Recognition* 37(2), 211–226.

H. R. Lourenço, O.C. Martin, and T. Stützle. (2003). "Iterated Local Search." In F. Glover and G. Kochenberger, (eds.), *Handbook of Metaheuristics*, Kluwer Academic Publishers, pp. 321–353.

J. Luck, C. Little, and W. Hoff (2000). "Registration of Range Data Using a Hybrid Simulated Annealing and Iterative Closest Point Algorithm. In *Proceedings of the IEEE Intl. Conf. on Rob. and Auto.*, San Francisco, USA, pp. 3739–3744.

R. Martí. (2003). "Multi Start Methods." In F. Glover and G. Kochenberger (eds.), *Handbook of Metaheuristics*, Kluwer Academic Publishers, pp. 355–368.

O. Monga, S. Benayoun, and O.D. Faugeras. (1992). "Using Partial Derivatives of 3D Images to Extract Typical Surface Features." In *Proceedings of the IEEE Computer Vision and Pattern Recognition (CVPR 92)*, Illinois (USA): Urbana Champaign, pp. 354–359.

Simunic, K. and S. Loncaric. (1998). "A Genetic Search-Based Partial Image Matching." *Proceedings of the 2nd IEEE International Conference on Intelligent Processing Systems (ICIPS 98)*, Australia: Gold Coast, pp. 119–122.

J. P. Thirion and A. Gourdon. (1996). "The 3-D Marching Lines Algorithm: New Results and Proofs." *Graphical Models and Image Processing* 58(6), 503–509.

S.M. Yamany, Ahmed, M.N. and A.A. Farag. (1999). "A New Genetic-Based Technique for Matching 3D Curves and Surfaces." *Pattern Recognition* 32, 1817–1820.

Z. Zhang. (1994). "Iterative Point Matching for Registration of Free-Form Curves and Surfaces." *International Journal of Computer Vision* 13(2), 119–152.